Vibrational Spectroscopy 131 (2024) 103662

Contents lists available at ScienceDirect

Vibrational Spectroscopy

journal homepage: www.elsevier.com/locate/vibspec

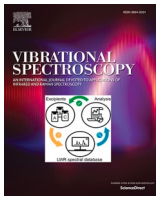

Evaluating the detection of cocaine and its impurities concealed inside fruit- and vegetable- food products using handheld spatially offset Raman spectroscopy

Sulaf Assi [a,*,1], Ismail Abbas [b,1], Leung Tang [c,1], Sarah Rowlands [a,1], Megan Wilson [a,1], Thomas Coombs [d,1], Basel Arafat [e,1], Mana Al-Hamid [f,1], Dhiya Al-Jumeily [a,1]

[a] Liverpool John Moores University, James Parson Tower, Liverpool L3 3AF, UK
[b] Faculty of Science, Lebanese University, Beirut, Lebanon
[c] Agilent Technologies, Field Detection Group, OX11 0RA, UK
[d] University Hospital Dorset, NHS, UK
[e] Anglia Ruskin University, Bishops Hall Lane, Chelmsford CM1 1SQ, UK
[f] Forensic Medical Service Centre in Najran, Najran, Saudi Arabia

ARTICLE INFO

Keywords:
Drugs
Cocaine
Food products
Handheld Raman
Spatially offset Raman spectroscopy
Algorithms

ABSTRACT

This study investigated the use of handheld spatially offset Raman spectroscopy for the identification of drugs concealed within fruit and vegetable food products, which is a common method of drug trafficking in busy environments such as airports. Handheld Raman spectroscopy is advantageous due to its mobility, speed, and chemical specificity for drug analysis. In this study, spatially offset Raman spectra of six substances were collected and included cocaine and its impurities. Raman spectra were collected for drugs on their own and for drugs concealed in transparent bags and in various food products such as green pepper, pomegranate, potato, and zucchini. The collected spectra were analyzed using different algorithms. The results showed successful identification of drugs in three out of the four tested food products, except for pomegranate, which had a thick rind and spongy tissue that hindered detection. An instrumental hit quality index algorithm provided instant identification with matches above 80% in the three identified products. Correlation in wavelength space yielded high correlation coefficient values between substances in food substrates and reference substances, although there were a few false negatives due to noisy spectra. Principal component analysis successfully differentiated between drugs in different food products. In summary, the study demonstrated the potential of handheld spatially offset Raman spectroscopy for identifying drugs concealed within food products. Future work aims to expand the technique to a wider range of substances and food products and develop a quantitative approach to predict substances' concentrations. Overall, this research contributes to the field of forensic applications and offers insights into the detection of illicit drugs in challenging scenarios.

1. Introduction

The change in the global supply chain over the last few years had its disadvantages. Hence, consumers could order any product via the Internet without any checks [1]. This in turn has given rise to the spread of sales of illegal drug products that can be trafficked across countries. Trafficking of illegal products has been affecting the safety and security of individuals globally especially with adulterated drug products. One of the dangerous aspects of illegal drug trafficking in adulterated products is the short- and long-term harm as well as death cases linked to adulterated drugs. The situation affects many people where everyday tons of illegal drugs are trafficked across nations prior to distribution of drug dealers and users within countries [1,2].

One way of concealing drugs prior to transport across countries is via food products and beverages. Foods and beverages have been adulterated with illicit drugs to enable criminal activities. For instance, illicit substances (including 3,4-methylenedioxymethamfet-amine, ketamine, mephedrone and nitrazepam) have been mixed with beverages, sweets,

* Corresponding author.
E-mail address: s.assi@ljmu.ac.uk (S. Assi).
[1] All authors contributed equally to the work.

https://doi.org/10.1016/j.vibspec.2024.103662
Received 19 June 2023; Received in revised form 23 January 2024; Accepted 28 January 2024
Available online 1 February 2024

milk tea, snacks, coffee and herbal tea packs [2]. According to recent data, significant amounts of cocaine powder have been processed in Europe from intermediary goods including coca paste and cocaine base. Some of these had been transported illegally from South America in materials such as charcoal and plastic, and were afterwards extracted in facilities with the necessary equipment [3]. Additional frequent methods for concealing drugs included drug packaging in fresh products such as green pepper [4], pineapples and bananas [5], pomegranates [6], fresh avocados [7], potatoes [8], squid [9] and zucchini [10].

Consumption of drugs of abuse has been causing serious problems to societies such as health problems, criminal activities and disruptions in cross-border trade [11,12]. In 2021 in the EU, 2.0 million adults used amfetamine derivatives, 2.6 million adults used 3,4-methylenedioxymethamfetamine, and 3.5 million adults used cocaine, emphasising the high proportion of the EU population at risk [11]. Thus, there is a societal need to reduce the intake of illegal drugs. This could be done by preventing the entry of illegal substances, blocking manufacturing locations and increasing public awareness about drugs' risks especially for widespread street drugs such as cocaine [13,14]. Hence, cocaine is used by about 17 million individuals worldwide [15].

Increased global cocaine production [15] and sophisticated trafficking methods (such as concealment in products) introduce a challenge to police officers, customs and/or forensic institutions in seizures of samples containing these products. Consequently, it is crucial to analyse drugs and food products transported across borders to mitigate their effects.

Reported conventional laboratory procedures for analysis of drugs and food products include colour tests, gas chromatography mass spectrometry, high performance liquid chromatography, liquid chromatography mass spectrometry and nuclear magnetic resonance [16–22]. Most of these techniques have high specificity, good sensitivity, flexibility with various matrices, quantitative analysis and extensive libraries. However, these techniques are often destructive, time-consuming and require extensive sample preparation and/or operators' training [16–23]. New techniques are thus required to deliver rapid screening tests with a high degree of sensitivity and specificity. On the other hand, Raman spectroscopy, which is based on inelastic light scattering, enables quick, affordable and non-destructive analysis [24,25]. It is often employed to give drugs a unique structural fingerprint that can used to identify them [26,27]. Raman spectroscopy is water-insensitive particularly in the range of 250–2000 cm^{-1} that is deployed in this study. This makes Raman spectroscopy suitable for analysis of moist materials (including illicit drugs) with minimal interference from water. Portable Raman spectroscopy provides quick, sensitive, non-destructive analysis of samples at the site they are encountered [28,29].

Subsequently, portable Raman spectroscopy has been used in previous studies for identifying cocaine concealed in drinks and clothing [30–35]. However, none of the aforementioned studies have used complicated matrices such as vegetable substrates and this was due to the nature of conventional Raman (CR) spectroscopy being a surface technique and that introduced in measuring samples through barriers.

In response to this challenge, SORS has recently been developed and enabled measuring samples across barriers [36–38]. In SORS mode, the emission is collected at a separate point from the laser excitation point and that enables collection of Raman spectra beyond the surface [36]. SORS has multiple uses, including identification of pharmaceutical raw materials in opaque containers, detection of explosives at airport screening checkpoints, detection of drugs at points of entry and detection of hazardous compounds in remote areas [36–38]. The popularity of SORS was due to the fact that it could detect substances several millimeters inside barriers [39,40]. SORS does not require direct contact and does not require any specific understanding of the nature of a container or barrier. It is worth mentioning here that SORS cannot detect substrates inside metallic barriers. Yet despite the latter disadvantage, SORS still offers quick and non-destructive analysis of majority of samples avoiding sample contamination and preserving the integrity of the samples [39–41],

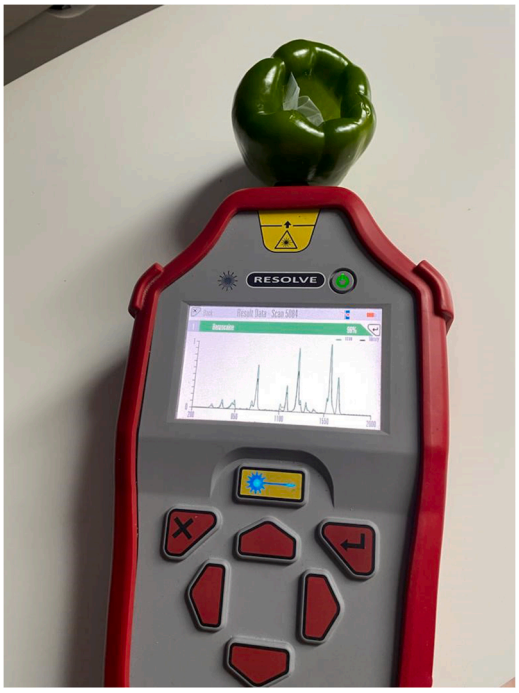

Fig. 1. Detection of benzocaine inside green pepper using the handheld Agilent spatially offset Raman spectrometer equipped with 830 nm laser wavelength.

An increased understanding of SORS use in various real-world circumstances will play a significant role in the general adoption of SORS. In this study, we present the use of SORS for identifying of substances (cocaine and its impurities) concealed in fruits- and vegetable-food products.

2. Materials and methods

2.1. Materials

Standard reference materials corresponding to cocaine hydrochloride (HCl) and its impurities were purchased from Sigma Aldrich and included benzocaine, calcium carbonate, cocaine hydrochloride, lidocaine, paracetamol, procaine HCl and sodium bicarbonate. For fruit- and vegetable- food products, one fruit and three vegetables were purchased from an off-license shop and included pomegranate, green pepper, potato and zucchini.

2.2. Instrumentation

Raman spectra were collected using the Agilent handheld SORS instrument equipped with 830 nm laser wavelength, 475 mW laser, spectral resolution of 15 cm^{-1} and laser spot size of 1 mm. The instrument was of light weight (2.2 kg) and had long battery lifetime (up to six hours). SORS mode allowed collection of light at 45 degrees from the incident laser light. This in turn allowed collection of Raman signal away beyond the sample surface [39].

2.3. Procedure

Pure substances of drugs/impurities were stored in transparent bags prior to measurement. For substances concealed in vegetable- and food-products (substrates), the transparent polyethylene bag containing the substance was placed inside the emptied substrate prior to SORS measurement. Hence a hole was made in each substrate using a zucchini

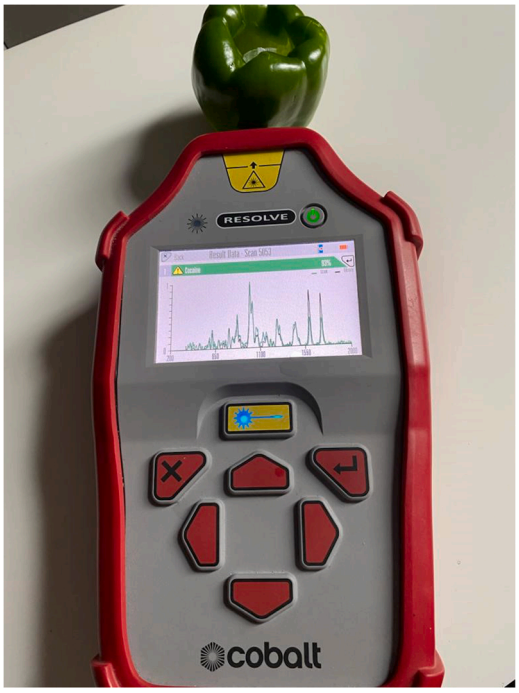

Fig. 2. Detection of cocaine hydrochloride inside green pepper using the handheld Agilent spatially offset Raman spectrometer equipped with 830 nm laser wavelength.

corer in order imitate real-life reported scenarios [3,4]. Then, the transparent polyethylene bag containing about 500 mg of each substance (in pure form) was placed inside the skin of the substrate so not to destroy the powder. This created two barriers for the drug the first bring the substrate and the second the transparent polyethylene bag (Figs. 1 and 2).

It is worthnoting to mention that each substance was kept inside the same polyethylene bag before placing this bag in different vegetables. The external of the polyethylene bag was cleaned with isopropanol wipes then dried prior to placing it inside each substrate. The thickness of the barriers varied depending on the substrate the substance is placed in. Pomegranate showed the thinnest barrier of 7 mm thickness, followed by green pepper that had about 10 mm thickness. On the other hand, courgette and potato thickness were around 15 mm. The polyethylene bag thickness was 100 μm for all the bags used in this study.

The through-barrier scan option was utilised for scanning substances inside (a) transparent bags, pomegranate, potato, green pepper and zucchini (Figs. 1 and 2). The through-barrier scanned enabled scanning in SORS mode that different from conventional Raman (CR) mode in the position of the incident and detected signal [2]. In CR mode (named as surface mode on the instrument), the Raman signal is detected at the position of the incident light [2]. This in turn allow collection of Raman spectra from the surface of the sample. On the other hand, SORS combines Raman spectroscopy with diffuse scattering. Thus in SORS mode, the Raman signal is detected at the incident light and collected at an offset position from the incident light. This allows the detection of the signal at the surface and beyond the surface. For the purpose of this study signal beyond the surface was considered. Three spectra were collected per sample over the wavenumber range of 250 – 2000 cm^{-1}. For SORS collection, spectra were collected via the pointer attachment with offset position of 5.5, integration time of two seconds, accumulations of 10 and laser power of 450 mW. For CR collection, spectra were also collected via the pointer either by placing it in contact with the vegetable or with the polyethylene bag containing the powder with position of 0, integration time of 1 s, accumulation of 5 and laser power of 270 mW.

2.4. Data interpretation

The inbuilt identification algorithm was used for initial characterisation of each sample that was matched against the instrumental library substances using hit quality index (HQI) that provided percentage match regarding the similarity of the test spectrum to a reference library spectrum and/or spectra. Pure substances should yield 100% HQI value

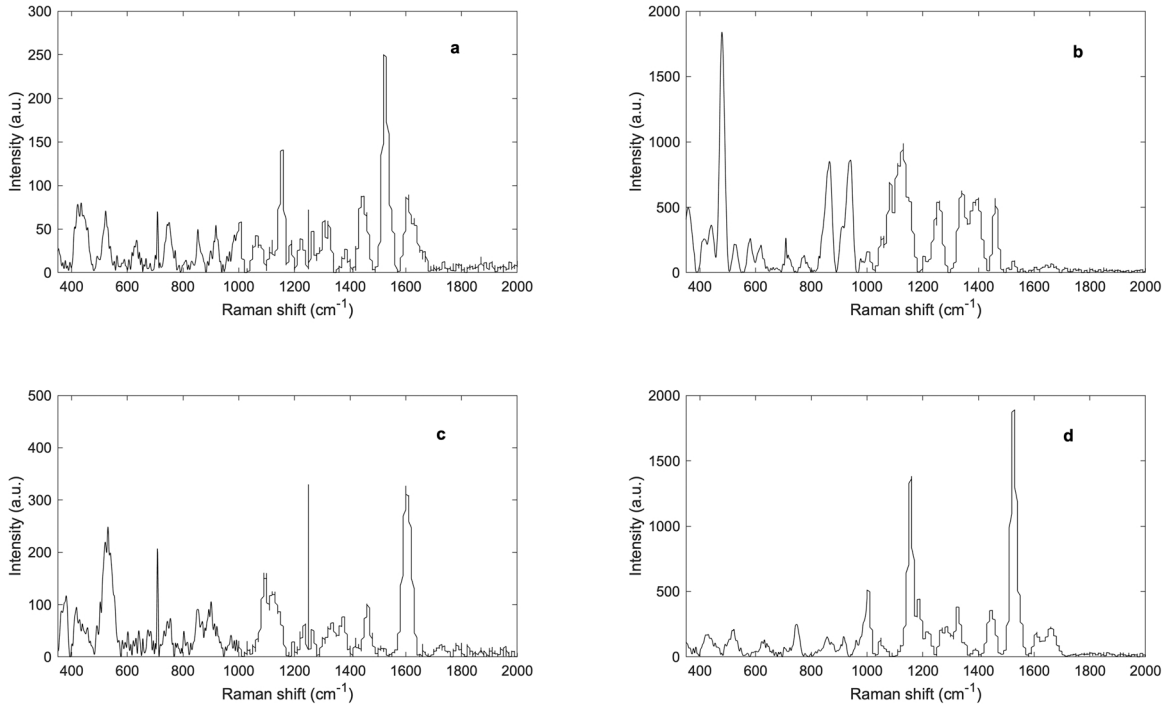

Fig. 3. Conventional Raman spectra of (a) green pepper, (b) potato; (c) pomegranate and (d) zucchini measured using the handheld Agilent Raman spectrometer equipped with 830 nm laser wavelength.

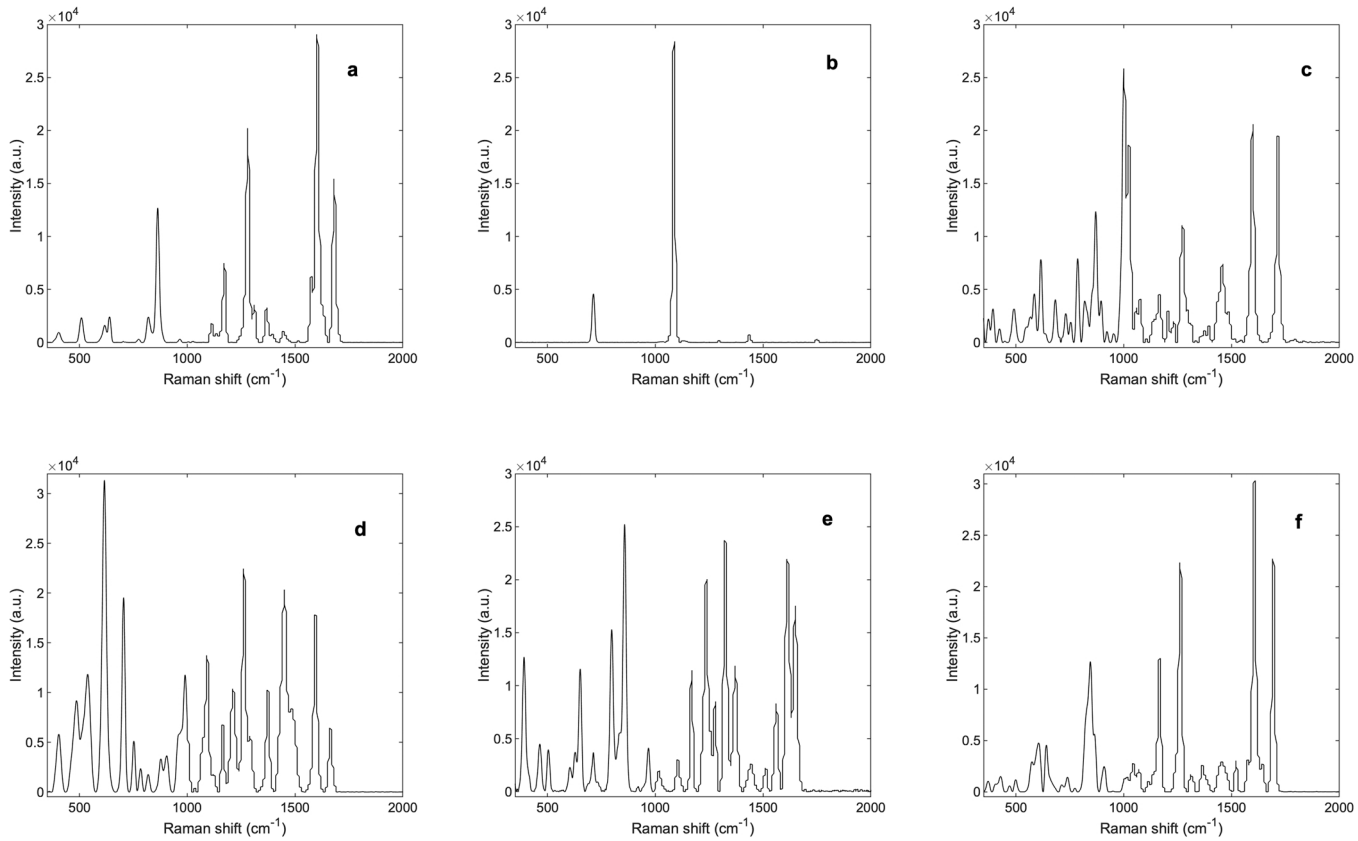

Fig. 4. Conventional Raman spectra of (a) benzocaine, (b) calcium carbonate; (c) cocaine hydrochloride, (d) lidocaine, (e) paracetamol and (f) procaine hydrochloride measured using the handheld Agilent Raman spectrometer equipped with 830 nm laser wavelength.

against their corresponding library reference.

Then spectra were exported into Matlab 2019b where spectral interpretation and machine learning analytics (MLAs) were applied. Spectral interpretation involved assigning functional groups corresponding to the sample measured against the literature. In addition, two MLAs were applied to the spectra in order to explore patterns among data and were correlation in wavenumber space (CWS) and principal component analysis (PCA). CWS method provided a correlation coefficient (r) value between spectra of different samples (library spectrum and test spectrum). An r value of − 1 indicated dissimilarity, whereas an r value of + 1 indicated identical samples. In addition, PCA reduced the original spectra into scores and loadings based on variance among the spectra. PC1 has the highest variance, PC2 the second highest variance not related to the first and so on… In this respect, plotting the first two or first three PC scores shows clusters among the measured samples according to the variances. To explore what these variances corresponded to, the PC loadings shows a spectrum similar to a Raman spectrum that in turns correspond to bands of key functional groups.

3. Results and discussion

The results demonstrated the power of SORS in detecting substances inside three out of the four vegetable- and fruit-food products being: green pepper, potato and zucchini. However, it was not possible to detect substances inside pomegranate where the latter masked the signal of the substance placed inside it. Cocaine and its impurities could be identified green pepper and zucchini using both the in-built identification algorithm and offline analysis. Fig. 1 shows cocaine detected instantly using the in-built identification algorithm inside green pepper and zucchini respectively. It is noteworthy to mention that these food products showed Raman activity; yet the SORS mode allowed to collect Raman spectra corresponding mainly to the substance inside the vegetable rather than the vegetable itself.

3.1. Raman activity of food products

The four food products showed Raman activity with multiple scattering bands that corresponded to bioactive constituents within these substrates when measured in CR mode (Fig. 3). Hence, numerous bands were observed for the four products which scattering intensities ranged between 300 and up to 2000 arbitrary units.

Green pepper Raman activity was mainly related to the carotenoid Raman constituents, phenolic compounds and lipids. Key bands related to green pepper were observed at 1120, 1160, 1260, 1287, 1450, 1520, 1570 and 1600 cm^{-1}. The band around 1120, 1160 and 1260 cm^{-1} could be linked to the C-C central polyene chain of the carotenoids [42]. In addition, the bands at 1520 and 1570 cm^{-1} to the C═C stretching of the polyene chain of carotenoids [42]. The band at 1287 and 1450 cm^{-1} could be attributed to the CH_2 twisting vibration of lipids [43]. The bands at 1600 cm^{-1} could be linked to the COC and COH stretching of phenolic compounds [43].

Pomegranate spectrum was noisy and showed hot pixels that resulted from overreaction of neighbouring pixels. Neighbouring pixels' overreaction occur when the intensity of a pixel is affected by the intensity of its neighbour pixel and that causes changes in the Raman spectrum such as the sharp band seen in Fig. 3c. It is noteworthy to mention that the intensity of the sharp pixel is affected by the instrument spatial and spectral resolution as well as the fluorescence of the sample measured. Yet in this case, the effects were not marked for pomegranate where some bands could be assigned due to detecting tannins in the ring and in the spongy white tissue at the inside of the fruit [44]. Specifically, bands in the region of 1640 – 1350 cm^{-1} could be related to the ring stretching vibration modes [44]. Thus, the band at 1610 cm^{-1} was linked to C═C stretching of the aromatic ring and the one at 1357 cm^{-1} was related to

Table 1
Functional groups for substances detected inside transparent bags and food products.

Drug/impurity	Band position (cm^{-1})	Band intensity (arbitrary units)			Corresponding group
		Transparent bag	Green pepper	Zucchini	
Benzocaine	863	12692	13921.9	1137.9	C-O stretching
[51–53]	1170	7360.3	6944.5	532.1	in-plane H-C-H bending
	1280	20130.3	16585.9	1124	C-C/C-N/C-O stretching of aromatic ring
	1600	29069.1	19142.8	866.8	stretching and bending of aromatic ring/NH2 scissoring
	1680	15438.2	8657.1	337.6	C═O stretching
Calcium carbonate [51,54]	713	4584.6	694.7	486.3	in plane C-O bending
	1090	28219.4	3813.7	195.3	strong C-O stretching
Cocaine HCl	1001	25607.2	493.4	353.3	symmetric stretching/breathing of the aromatic ring
[53,55–59]	821	3841.3	87	55.6	C-C stretching of the tropane ring
	870	12351.8	197	127.8	C-C stretching of the tropane ring
	897	3759.8	72.5	53.1	C-C stretching of the tropane ring
	1210	2958.8	none	114.9	C-N stretching
	1460	7285.9	173.8	74.5	asymmetric CH3 deformation
	1490	2690.3	none	20.2	C-C stretching
	1599	20591.2	223.3	90.2	C═C stretching of the aromatic ring
	1600	20591.2	223.3	90.1	C═C stretching of the aromatic ring
	1735	19466.5	none	39.5	C═O asymmetric stretching
Lidocaine [52,60,61]	957	5545.2	none	none	C-C stretching
	990	11770.1	463.1	286.8	C-C stretching
	1090	13685.8	399.7	331.9	C-C/C-N stretching of aromatic ring
	1160	6636.9	238.8	146.9	C-N stretching
	1260	22093	646.1	519.5	C-O stretching (alkyl aryl ether)
	1370	9727	315.2	228.9	CH_2 twisting
	1450	1884	520.8	1450	C-N stretching and N-H bending
	1490	8334.2	none	none	C-N stretching and N-H bending
	1600	17315.5	383.5	243.9	C-H wagging
	1670	6260.2	134.5	59.9	C═C stretching
Paracetamol [62–64]	798	15297	1716.8	165	C-N-C ring stretching
	832	5473.5	none	56.6	C-H bending out-of-plane
	858	25221.5	2846.9	297	C═C bending
	1170	10529.8	1122	32	C-C ring stretching
	1240	19784.9	2107.9	106.9	Stretching of benzene -OH
	1280	8383.7	803.9	80.9	Amide III stretching
	1320	23709.1	2150.3	93.4	S═O stretching (sulfon)
	1370	10780.5	916.5	174.1	S═O stretching (sulfonate)
	1510	2238.5	none	none	Amide II stretching
	1560	7605.9	453.1	64.7	Aromatic ring stretching
	1610	21680.4	1325.6	14.1	Amide I stretching
	1650	15738.3	937.3	none	C+C stretching
Procaine HCl [65,66]	644	4214.1	733.7	361.2	C-C-C bending
	707	497.6	none	72.4	C-C-C stretching
	741	1376.4	194.7	94.6	C-H stretching
	845	12689.5	1778.6	963.7	C-H stretching
	866	5461.2	none	477	C-H out-of-plane wagging
	1040	2646.2	349.3	none	C-H stretching
	1170	13007.8	2039.9	991.3	in-plane H-C-H bending
	1260	21740.4	3406.2	1564.7	C-H bending
	1360	2584.3	357.9	137.7	C-H bending
	1520	2150.8	305.8	68.4	asymmetric CH bending
	1570	2908.7	none	none	C-C stretching + C-C-O stretching + NH2 bending
	1690	22585.5	1927.2	509.1	C-O stretching
Sodium bicarbonate [67]	940	4404.1	91.2	60	C-O stretching
	1020	4072.9	none	none	HCO_3 stretching
	1040	16442.8	278.4	123	C-O stretching
	1100	1859.4	none	none	C-O stretching
	1270	6649.5	189.9	90.3	O-C-O symmetric stretching

HCl: hydrochloride.

the C═C and C-O-C stretching [44]. Another band was featured at 530 cm^{-1} and related to the C-C bending of the benzopyrylium ring [45].

Potato showed better Raman scattering over pomegranate despite some fluorescence and this was mainly related to carbohydrates, protein and aliphatic fatty acids constituents. Characteristic bands for carbohydrates in potatoes were seen at 417, 437 and 479 cm^{-1} and were linked to C-C-O and C-C-C deformations that were related to glycosidic ring skeletal deformations, bending C-C-C + twisting C-O, scissoring of C-C-C and out-of-plane C-O and C-O-C glycosidic stretching [46,47]. Complex carbohydrate features in potato were also observed between 970 and 1190 cm^{-1} as well as 1200 - 1410 cm^{-1} [48]. In this respect, bands at 909, 936, 1080 and 1130 cm^{-1} were related to C-O-C symmetric in plane stretching, C-O-H bending, C-O stretching + C-C stretching + C-O-H bending and CH_2OH stretching respectively [47]. Moreover, bands at 1260, 1340 and 1400 cm^{-1} were linked to aromatic C-O stretching, C-O stretching and C-O-H bending and CH_2 deformation respectively [47]. The band at 1441 cm^{-1} could be related to the C-H bending vibration of the CH_2 group of the aliphatic fatty acids present in potatoes [48].

Zucchini showed Raman activity related to plastocyanin, beta-carotene and carbohydrate constituents. Plastocynanin-related bands were attributed to the Cu-S stretch and were seen at 421 and 518 cm^{-1} [49]. Carbohydrate related bands were seen between 1000 and 1200 cm^{-1} and corresponded to C-CH_3 rocking (1000 cm^{-1}) and C-C

stretching (1160 and 1190 cm^{-1}). Additional bands were seen at 1450 and 1530 cm^{-1} that corresponded to CH_3 bending and C═C stretching of beta-carotene [50].

3.2. Raman activity of substances

Most substances, apart from calcium carbonate, showed strong Raman scattering within the wavenumber range of 400 – 1800 cm^{-1} (Fig. 4).

Hence, calcium carbonate showed only two Raman bands at 713 (weak) and 1090 (strong) cm^{-1} that corresponded to in-plane C-O bending and C-O stretching respectively. It is worthnoting to mention here that the intensity of calcium carbonate strong band was 28,219 arbitrary units. The remaining substances also showed strong bands with intensity around 30,000 arbitrary units yet had numerous bands. Hence, the number of bands for the remaining substances ranged between 17 bands (observed for benzocaine) and 33 bands (observed for cocaine HCl). Lidocaine, paracetamol and procaine HCl showed 21, 24 and 30 bands respectively.

Benzocaine showed key bands attributed to C-O stretching (863 cm^{-1}), in-plane H-C-H bending (1170 cm^{-1}), C-C/C-N/C-O stretching of aromatic ring (1280 cm^{-1}), stretching and bending of aromatic ring/NH_2 scissoring (1600 cm^{-1}) and C═O stretching (1680 cm^{-1}). Cocaine HCl showed bands related to the symmetric stretching/breathing of the aromatic ring (1001 cm^{-1}), C═C stretching of aromatic ring (1599 and 1600 cm^{-1}), C-C stretching of the tropane ring (821, 870 and 897 cm^{-1}), C-N stretching (1210 cm^{-1}), asymmetric CH_3 deformation (1460 cm^{-1}), C-C stretching (1490 cm^{-1}) and C═O stretching (1735 cm^{-1}). Lidocaine bands were linked to C-C stretching (957 and 990 cm^{-1}), C-C/C-N stretching of the aromatic ring (1090 cm^{-1}), C-N stretching (1160 cm^{-1}), C-O stretching (1260 cm^{-1}), CH_2 twisting (1370 cm^{-1}), C-N stretching and N-H bending (1450 and1490 cm^{-1}), C-H wagging (1600 cm^{-1}) and C═C stretching (1670 cm^{-1}).

Paracetamol key bands were attributed to C-N-C ring stretching ((798 cm^{-1}), C-H out of plane bending (832 cm^{-1}), C═C bending (858 cm^{-1}), C-C ring stretching (1870 cm^{-1}), stretching of OH group of benzene ring (1240 cm^{-1}), stretching of amide I, II and III (at 1610, 1510 and 1280 cm^{-1}), S═O stretching of sulfone and sulfonate (at 1320 and1370 cm^{-1}) and aromatic ring stretching (at 1560 cm^{-1}). Procaine HCl showed bands corresponding to C-C-C bending and stretching (644 and 707 cm^{-1}), CH stretching (741, 845 and 1040 cm^{-1}), CH bending (1260, 1360 and 1520 cm^{-1}), in-plane H-C-H bending (1170 cm^{-1}), C-C stretching + C-C-O stretching + NH_2 bending (1570 cm^{-1}) and C-O stretching (1690 cm^{-1}).

3.3. Detection of substances inside food products

For evaluating the detection of substances inside food products, substances were placed inside transparent bags that was in turn placed inside the food product. In this respect, pomegranate masked the signal of the substance(s) inside it that could not be detected. Inside potato, only three out of the six substances could be detected and were benzocaine, lidocaine and paracetamol.

On the other hand, all substances could be detected inside green pepper and zucchini yet the degree of interference varied depending on the Raman activity of the substance measured (Table 1). All benzocaine, calcium carbonate and cocaine bands could be detected inside green pepper and zucchini; whereas, only few bands could not be detected for lidocaine, paracetamol and procaine HCl inside these vegetables. It is worthnoting that substances detected inside vegetables had lower intensity than when measured inside transparent bags and that could be related partly to the interreference from the food product and partly from the weak Raman signal inside of the sample.

Table 2
HQI values obtained using the instrument in-built algorithm.

Substance	CAS number	Description	Container	Match	HQI (%)
Benzocaine	94-09-7	white powder	Transparent bag	benzocaine	98
Calcium carbonate	471-34-1	white powder	Transparent bag	Calcium carbonate	100
Cocaine HCl	53-21-4	white powder	Transparent bag	cocaine	99
Lidocaine	137-58-6	white powder	Transparent bag	lidocaine	90
Paracetamol	103-90-2	white powder	Transparent bag	paracetamol	100
Procaine HCl	51-05-8	white powder	Transparent bag	procaine HCl	98
Green pepper	NA	green vegetable	None	palm oil	84
Zucchini	NA	light green vegetable	None	palm oil	83
Benzocaine	94-09-7	white powder	Green pepper	benzocaine	95
Calcium carbonate	471-34-1	white powder	Green pepper	calcium carbonate	99
Cocaine HCl	53-21-4	white powder	Green pepper	Cocaine+palm oil	92
Lidocaine	137-58-6	white powder	Green pepper	lidocaine	83
Paracetamol	103-90-2	white powder	Green pepper	paracetamol	94
Procaine HCl	51-05-8	white powder	Green pepper	procaine HCl	88
Benzocaine	94-09-7	white powder	Zucchini	benzocaine + Sodium-p-nitrophenolate	91
Calcium carbonate	471-34-1	white powder	Zucchini	calcium carbonate	98
Cocaine HCl	53-21-4	white powder	Zucchini	cocaine+ 5-methoxy-2-methyl-4-nitroaniline	90
Lidocaine	137-58-6	white powder	Zucchini	lidocaine	81
Paracetamol	103-90-2	white powder	Zucchini	paracetamol	90
Procaine HCl	51-05-8	white powder	Zucchini	procaine HCl	84

HQI: hit quality index.

3.4. Classification of substances inside food products

The detection of substances inside food products was featured in the in-built identification results (Table 2). The in-built identification was applied by matching the test spectrum against the spectral library. Thus, the library content, alongside the hit quality (HQI) index contributed to the accuracy of the match value obtained. It is worthnoting that HQI is based on correlation coefficient value yet yields a % match where 100% denotes identical match and 0% indicates a mismatch. The threshold adopted for HQI in this research was 95% [32].

Inside transparent bags, all substances matched their library reference with an HQI value > 98%. Yet inside food products, the result was slightly lower for green pepper and zucchini in which the HQI values of substances gave variable matches with values > 80% for a reference library substance or mixture. Hence, benzocaine in green pepper gave 95% match against benzocaine library signature and 91% match against a mixture of benzocaine and sodium-p-nitrophenolate. Calcium carbonate, lidocaine, paracetamol and procaine inside green pepper and zucchini only matched their library reference but gave match values in the range of 81–99%. On the other hand, cocaine HCl gave matches to mixtures that were cocaine + palm oil and cocaine+ 5-methoxy-2-methyl-4-nitroaniline that had HQI values of 92% and 90% respectively.

Subsequently to get more conclusive results, offline analysis was

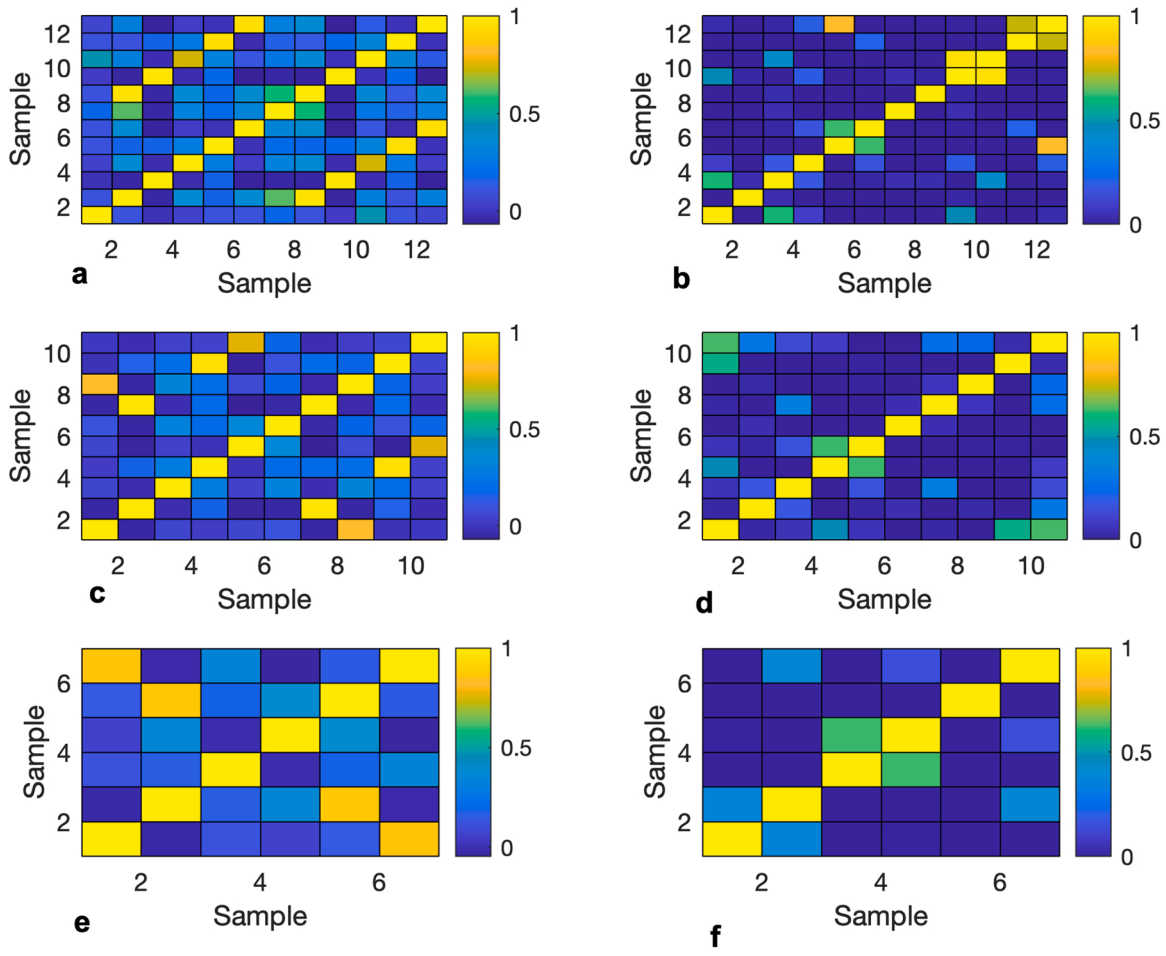

Fig. 5. Correlation and probability based maps of the Raman spectra of (1) vegetable substrate (green pepper, zucchini or potato), (2) benzocaine, (3) calcium carbonate, (4) cocaine hydrochloride, (5) lidocaine, (6) paracetamol, (7) procaine hydrochloride, (8) benzocaine inside green pepper, (9) calcium carbonate inside green pepper, (10) cocaine hydrochloride inside green pepper, (11) lidocaine inside green pepper, (12) paracetamol inside green pepper, (13) procaine hydrochloride inside the substrate being green pepper (a and b), zucchini (c and d) and potato (e and f)measured using using the handheld Agilent spatially offset Raman spectrometer equipped with 830 nm laser wavelength.

made using CWS and PCA (Figs. 5 and 6). Both CWS and PCA compared the Raman spectra of the substances in transparent packaging to the Raman spectra of the substances inside green pepper, zucchini and potatoes.

The results varied between green pepper, zucchini and potatoes. Inside green pepper, five out of the six substances showed r values > 0.95 against their reference standard spectrum. Hence, only benzocaine inside green pepper showed an r value of 0.93 against its library reference and this could be related to noise in both spectra rather than band positions. Hence, both benzocaine and benzocaine in green pepper showed matching band positions (Appendix I). Benzocaine inside zucchini was noisy so was excluded from the correlation map. Four out of the remaining substances inside zucchini showed r values > 0.95 remaining substances apart from lidocaine in zucchini that showed slightly lower match against its reference standard despite the presence of the majority of lidocaine bands. Hence, the latter false negative error could be related to noise in the spectrum of lidocaine inside zucchini. Noise in Raman spectra of substances inside vegetables could be attributed to fluorescence of carbohydrates and chlorophyll that were constituents of zucchini. Carbohydrates were also major constituents in potato and that contributed to noise in spectra of substances placed inside potatoes. Hence, all three substances spectra inside potato were suitable for analysis and were benzocaine, lidocaine and paracetamol. Of these three substances, benzocaine and lidocaine inside potatoes showed r values > 0.95 against their corresponding reference standard spectrum in contrary to paracetamol despite its Raman activity. These findings showed a limitation in CWS method that was affected by noise in samples' spectra and/or fluorescence attributed to food products themselves. This was because CWS measured the momentum product between full Raman spectra considering the bands and the noise encountered in spectra. In this specific case, it was not possible to exclude data based on low noise that was encountered over the full Raman spectra of the analytes.

Consequently, PCA was applied as this algorithm was based on the variance among the dataset and hence it offered the option to choose variances corresponding to the bands rather than the noise among the spectra of the samples measured. Three PCA models were constructed on the same samples to which CWS was applied (Fig. 6).

In this respect, PCA model 1 was applied to Raman spectra of the six substances measured in transparent bags, inside green pepper and to green pepper on its own. The first three PCs accounted for 78.5% of the variance among the spectra as follows: PC1 36.9%, PC2 25.8% and PC3 15.8%. The loading on PC1 (36.9%) showed contribution mainly from lidocaine in transparent bag that showed the highest variance among the data. The PC scores showed distinct grouping between drugs inside green pepper and drugs in transparent bags apart from benzocaine (Fig. 6a). Hence, benzocaine scores were grouped together whether in transparent bag or inside the green pepper. This complemented CWS results that could not identify benzocaine inside green pepper. Nonetheless, the remaining drugs inside green pepper were clustered with

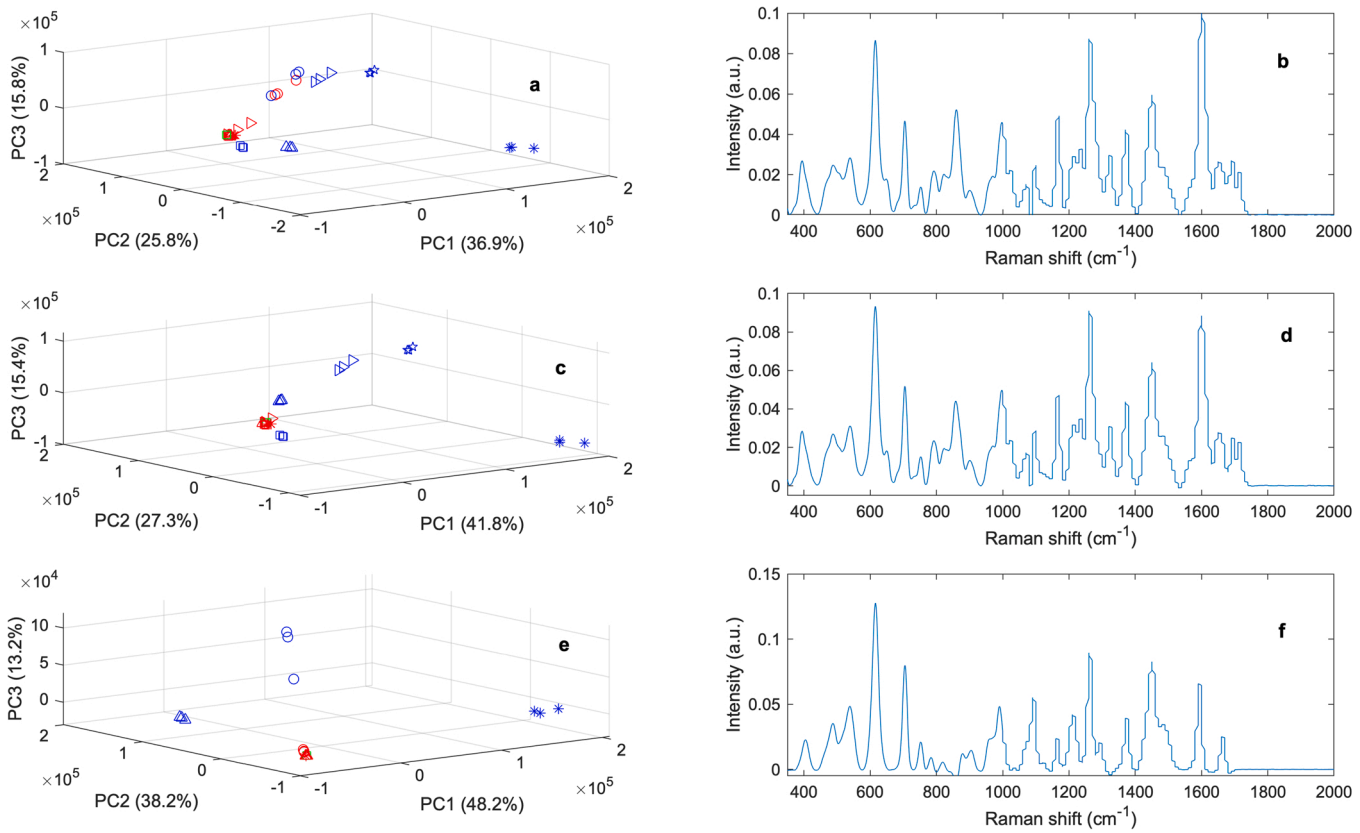

Fig. 6. PCA scores and loading plots of drugs in green pepper model (a) and (b), drugs in zucchini model (c) and (d) and drugs in potato model (e) and (f) such that: Green pepper, zucchini and potato are denoted as green squares in a, c and e respectively. Drugs are denoted as: benzocaine (blue circle), calcium carbonate (blue square), cocaine hydrochloride (blue pentagon), lidocaine (blue asterisk),.

green pepper and that confirmed the importance of the substrate that the substance had been placed in. Similar patterns were seen in PCA models 2 and 3 that were applied to substances in zucchini and potato. Hence, PCA model 2 applied to substances in zucchini showed two distinct groups between substances in zucchini and substances in transparent bags (Fig. 6b). The first three loadings of PCA model 2 contributed to 84.5% of the variance as follows: PC1 48.2%, PC2 27.3% and PC3 15.4%. The highest variance (i.e. PC1) was linked as well to lidocaine scores that showed the highest variance among the data. Similarly, PCA model 3 showed two distinct groups for the substances inside potatoes and those in transparent bags. The first three PCs of model 3 contributed to 99.6% of the variance among the spectra as such: PC1 48.2%, PC2 38.2% and PC3 13.2%. PC1 loading of model 3 was also linked to lidocaine as in previous models where lidocaine scores showed the highest variance among the substances scores. Therefore, PCA algorithm provided distinct groups relating to the packaging of the drugs; whereas, the combination of the instrument inbuilt algorithm and CWS was successful in identifying the drug itself. Thus, the three algorithms showed to be complementary in identifying drugs inside vegetables.

4. Conclusions

In summary, handheld SORS offered a rapid and accurate technique for locating drugs/drug impurities concealed inside vegetable- and fruit-food products. However, the results varied depending on the substance itself and the Raman activity/fluorescence of the food product. Hence, food products represent complex mixtures of carbohydrates, proteins, vitamins and lipids that in turn could interfere with the Raman activity of the measured substance. However, this Raman activity and the position of the bands could be affected by the instrumental settings including laser wavelength used and laser power. For instance, increased laser power can result in overheating of the sample that can cause shift in the band position and possibly more fluorescence that features in the Raman spectrum of the sample.

Though SORS has the ability to measure through barriers and analytes certain interference(s) could still be encountered from the surface. Nonetheless using suitable chemometric algorithm(s), this interference could be eliminated. In the present study, the combination of three algorithms were successful for determining drugs/impurities in three food products. These algorithms were the hit quality index that was the instrument in-built algorithm, CWS and PCA. The three algorithms were complementary in identifying the substances detected as well as the matrix being green pepper, zucchini and potatoes. On the contrary, drugs/impurities could not be detected inside pomegranate and that could be linked to the opaque nature of the fruit skin. That introduced a limitation in the study that could be addressed by using transmission Raman spectroscopy. Further limitations could be encountered when applying the method to street drug samples that contain multiple impurities and hence impose an additional challenge in identification. Moreover, the amount per substance available was low (few gram per substance) and this did not allow investigating maximum depth that could be detected with SORS. Therefore, future work should address these lmitiations and consider more quantitative approach applied to SORS spectra of substances inside vegetables. In addition, detecting drugs inside different analytes (e.g. toys) and food products (e.g. milk and baking powder) can further contribute to the literature regarding forensic analysis.

CRediT authorship contribution statement

Arafat Basel: Writing – review & editing, Validation, Investigation, Formal analysis, Conceptualization. **Al-Hamid Mana:** Writing – review

& editing, Validation. **Al-Jumeily Dhiya:** Writing – review & editing, Visualization, Validation, Project administration, Methodology, Formal analysis, Data curation, Conceptualization. **Tang Leung:** Writing – review & editing, Visualization, Validation, Software, Conceptualization. **Wilson Megan:** Writing – review & editing, Validation, Investigation. **Coombs Thomas:** Writing – review & editing, Visualization, Validation. **Rowlands Sarah:** Writing – review & editing, Validation. **Assi Sulaf:** Writing – review & editing, Writing – original draft, Methodology, Formal analysis, Data curation, Conceptualization. **Abbas Ismail:** Writing – review & editing, Writing – original draft, Visualization, Validation, Formal analysis, Data curation.

Declaration of Competing Interest

The authors declare that they have no known competing financial interests or personal relationships that could have appeared to influence the work reported in this paper.

Data availability

No data was used for the research described in the article.

Acknowledgements

The eSystem Engineering Society for their support with data analysis.

References

[1] M.S. Jenner, International drug trafficking: a global problem with a domestic solution, Indiana J. Glob. Leg. Stud. 18 (2) (2011) 901–927, https://doi.org/10.2979/indjglolegstu.18.2.901.
[2] C. Eliasson, N.A. Macleod, P. Matousek, Non-invasive detection of cocaine dissolved in beverages using displaced Raman spectroscopy, Anal. Chim. Acta 607 (1) (2008) 50–53, https://doi.org/10.1016/j.aca.2007.11.023.
[3] EU drug markets analyses from Europol and the EMCDDA. 2022. [Cited 2022 December 29]. Available from: ⟨https://www.europol.europa.eu/media-press/newsroom/news/2022-eu-drug-markets-analyses-europol-and-emcdda⟩.
[4] WGRZ, Drugs found inside a green pepper seized from Gowanda Correctional. 2020 May 5 [Cited 2022 December 29]. Available from: ⟨https://www.wgrz.com/article/news/crime/drugs-found-in-green-pepper-seized-from-gowanda-correctional/71–38ab70d1–1e66–4842-ac38–0edf7cccfcc4⟩.
[5] Mitchell M. Drugs find way into shipments of vegetables. The Baltimore Sun. 2000 May 21 [Cited 2022 December 29]. Available from: ⟨https://www.baltimoresun.com/news/bs-xpm-2000–05-21–0006020421-story.html⟩.
[6] Layla M., Aya I. Saudi Arabia bans Lebanese fruit and vegetable imports over drug smuggling concerns. The National. 2021 April 23 [Cited 2022 December 29]. Available from: ⟨https://www.thenationalnews.com/gulf/saudi-arabia/saudi-arabia-bans-lebanese-fruit-and-vegetable-imports-over-drug-smuggling-concerns-1.1209496⟩.
[7] Marcos O. Surgical Masks and Fruits Used to Transport Drugs Amid Coronavirus Pandemic. DIÁLOGO. 2020 April 14 [Cited 2022 December 29]. Available from: ⟨https://dialogo-americas.com/articles/surgical-masks-and-fruits-used-to-transport-drugs-amid-coronavirus⟩ pandemic.
[8] Diksha R. Colombian police seize 1,300 Kg cocaine camouflaged as potatoes: Report. NDTV. 2020 June 16 [Cited 2022 December 29]. Available from: ⟨https://www.ndtv.com/world-news/colombian-police-seize-1–300-kg-cocaine-camouflaged-as-potatoes-report-3072537⟩.
[9] Francesco G. Europe flooded with cocaine despite coronavirus trade disruptions. Reuters. 2020 April 30 [Cited 2022 December 29]. Available from: ⟨https://www.reuters.com/article/us-health-coronavirus-eu-drugs-idUSKBN22C1TY⟩.
[10] Sara N. Drug smugglers get creative - by hiding cocaine in Bermuda shorts and courgettes. Mailonline. 2009 August 19 [Cited 2022 December 29]. Available from: ⟨https://www.dailymail.co.uk/news/article-1207308/Cocaine-underpants-Smugglers-creative-hiding-drugs-Bermuda-shorts-courgettes.html⟩.
[11] European Monitoring Centre for Drugs and Drug Addiction (EMCDDA). European Drug Report 2021. Trends and Developments; Publications Office of the European Union: Luxembourg. [Cited 2022 December 29]. Available from: ⟨https://www.emcdda.europa.eu/publications/edr/trends-developments/2021_en⟩.
[12] United Nations Office on Drugs and Crime. World Drug Report 2021. Division for Policy Analysis and Public Affairs: Vienna, Austria. [Cited 2022 December 29]. Available from: ⟨https://www.unodc.org/unodc/en/data-and-analysis/wdr2021.html⟩.
[13] European Monitoring Centre for Drugs and Drug Addiction. The state of the drugs problem in Europe. 2010. [Cited 2022 December 29]. Available from: ⟨https://www.emcdda.europa.eu/publications/annual-report/2010_en⟩.
[14] United Nations Office on Drugs and Crime. World drug report. 2016. [Cited 2022 December 29]. Available from: ⟨https://www.unodc.org/wdr2016/⟩.
[15] UNODC. Market analysis of plant-based drugs - opiates, cocaine, cannabis. 2017. [Cited 2022 December 29]. Available from: ⟨https://www.unodc.org/wdr2017/field/Booklet_3_Plantbased_drugs.pdf⟩.
[16] U. Holzgrabe, NMR spectroscopy in pharmaceutical analysis, Elsevier,, 2017.
[17] Y. Song, Y. Cong, B. Wang, N. Zhang, Applications of Fourier transform infrared spectroscopy to pharmaceutical preparations, Expert Opin. Drug Deliv. 17 (4) (2020) 551–571, https://doi.org/10.1080/17425247.2020.1737671.
[18] U. Holzgrabe, R. Deubner, C. Schollmayer, B. Waibel, Quantitative NMR spectroscopy applications in drug analysis, J. Pharm. Biomed. Anal. 38 (5) (2005) 806–812, https://doi.org/10.1016/j.jpba.2005.01.050.
[19] Y. Shi, H. Dai, Y. Sun, J. Hu, P. Ni, Z. Li, Fluorescent sensing of cocaine based on a structure switching aptamer, gold nanoparticles and graphene oxide, Analyst 138 (23) (2013) 7152–7156, https://doi.org/10.1039/C3AN00897E.
[20] M.N. Stojanovic, P. De Prada, D.W. Landry, Aptamer-based folding fluorescent sensor for cocaine, J. Am. Chem. Soc. J. Am. Chem. Soc. 123 (21) (2001) 4928–4931, https://doi.org/10.1021/ja0038171.
[21] J. Zhang, L. Wang, D. Pan, S. Song, F.Y. Boey, H. Zhang, C. Fan, Visual cocaine detection with gold nanoparticles and rationally engineered aptamer structures, Small 4 (8) (2008) 1196–1200, https://doi.org/10.1002/smll.200800057.
[22] S.C. Cheng, Y.D. Tsai, C.W. Lee, B.H. Chen, J. Shiea, Direct and rapid characterization of illicit drugs in adulterated samples using thermal desorption electrospray ionization mass spectrometry, J. Food Drug Anal. 27 (2) (2019) 451–459, https://doi.org/10.1016/j.jfda.2018.12.005.
[23] Y. Tsumura, T. Mitome, S. Kimoto, False positives and false negatives with a cocaine-specific field test and modification of test protocol to reduce false decision, Forensic Sci. Int. 155 (2-3) (2005) 158–164, https://doi.org/10.1016/j.forsciint.2004.11.011.
[24] S.E. Bell, J.R. Beattie, J.J. McGarvey, K.L. Peters, N.M. Sirimuthu, S.J. Speers, Development of sampling methods for Raman analysis of solid dosage forms of therapeutic and illicit drugs, J. Raman Spectrosc. 35 (5) (2004) 409–417, https://doi.org/10.1002/jrs.1160.
[25] A.G. Ryder, G.M. O'Connor, T.J. Glynn, Quantitative analysis of cocaine in solid mixtures using Raman spectroscopy and chemometric methods, J. Raman Spectrosc. 31 (3) (2000) 221–227, https://doi.org/10.1002/(SICI)1097-4555(200003)31:3<221::AID-JRS518>3.0.CO;2-5.
[26] E.M.A. Ali, H.G.M. Edwards, The detection of flunitrazepam in beverages using portable Raman spectroscopy, Drug Test. Anal. 9 (2017) 256–259, https://doi.org/10.1002/dta.1969.
[27] M.J. West, M.J. Went, Detection of drugs of abuse by Raman spectroscopy, Drug Test. Anal. 3 (2011) 532–538, https://doi.org/10.1002/dta.217.
[28] D. Clark, C. Rodger, Discovery and Formulation, in: P. Matousek, M. Morris (Eds.), Emerging Raman applications and techniques in biomedical and pharmaceutical fields. Biological and medical physics, biomedical engineering, Springer, Berlin, Heidelberg, 2010.
[29] E.M. Ali, H.G. Edwards, M.D. Hargreaves, I.J. Scowen, In situ detection of cocaine hydrochloride in clothing impregnated with the drug using benchtop and portable Raman spectroscopy, J. Raman Spectrosc. 41 (9) (2010) 938–943, https://doi.org/10.1002/jrs.2518.
[30] C.A. de Oliveira Penido, M.T. Pacheco, I.K. Lednev, Jr.L. Silveira, Raman spectroscopy in forensic analysis: identification of cocaine and other illegal drugs of abuse, J. Raman Spectrosc. 47 (1) (2016) 28–38, https://doi.org/10.1002/jrs.4864.
[31] M.O. Amin, E. Al-Hetlani, I.K. Lednev, Detection and identification of drug traces in latent fingermarks using Raman spectroscopy, Sci. Rep. 12 (2022) 3136–3144, https://doi.org/10.1038/s41598-022-07168-6.
[32] J. Calvo-Castro, S.N. Tchakounte, V. Guarino, A.A. Ahmed, J.L. Stair, Flipped detection of psychoactive substances in complex mixtures using handheld Raman spectroscopy coupled to chemometrics, J. Raman Spectrosc. 53 (8) (2022) 1428–1444, https://doi.org/10.1002/jrs.6372.
[33] C.M. Liu, H.Y. He, L. Xu, Z.D. Hua, New qualitative analysis strategy for illicit drugs using Raman spectroscopy and characteristic peaks method, Drug Test. Anal. 13 (3) (2021) 720–728, https://doi.org/10.1002/dta.2963.
[34] R.F. Kranenburg, J. Verduin, R. de Ridder, Y. Weesepoel, M. Alewijn, M. Heerschop, et al., Performance evaluation of handheld Raman spectroscopy for cocaine detection in forensic case samples, Drug Test. Anal. 13 (5) (2021) 1054–1067, https://doi.org/10.1002/dta.2993.
[35] R.S. Das, Y.K. Agrawal, Raman spectroscopy: recent advancements, techniques and applications, Vib. Spectrosc. 57 (2) (2011) 163–176, https://doi.org/10.1016/j.vibspec.2011.08.003.
[36] W.J. Olds, S. Sundarajoo, M. Selby, B. Cletus, P.M. Fredericks, E.L. Izake, Noninvasive, quantitative analysis of drug mixtures in containers using spatially offset Raman spectroscopy (SORS) and multivariate statistical analysis, Appl. Spectrosc. 66 (5) (2012) 530–537, https://doi.org/10.1366/11-06554.
[37] C. Eliasson, P. Matousek, Noninvasive authentication of pharmaceutical products through packaging using spatially offset Raman spectroscopy, Anal. Chem. 79 (4) (2007) 1696–1701, https://doi.org/10.1021/ac062223z.
[38] W.J. Olds, E. Jaatinen, P. Fredericks, et al., Spatially offset Raman spectroscopy (SORS) for the analysis and detection of packaged pharmaceuticals and concealed drugs, Forensic Sci. Int. 212 (1-3) (2011) 69–77, https://doi.org/10.1016/j.forsciint.2011.05.016.
[39] P. Matousek, I.P. Clark, E.R. Draper, M.D. Morris, A.E. Goodship, N. Everall, M. Towrie, W.F. Finney, A.W. Parker, Subspatially probing in diffusely scattering media using spatially offset Raman spectroscopy, Appl. Spectrosc. 59 (4) (2005) 393–400, https://doi.org/10.1366/0003702053641450.

[40] N. Stone, R. Baker, K. Rogers, A.W. Parker, P. Matousek, Subspatially probing of calcifications with spatially offset Raman spectroscopy (SORS): future possibilities for the diagnosis of breast cancer, Analyst 132 (9) (2007) 899–905, https://doi.org/10.1039/B705029A.
[41] P. Matousek, M.D. Morris, N. Everall, I.P. Clark, M. Towrie, E. Draper, A. Goodship, A.W. Parker, Numerical simulations of subspatially probing in diffusely scattering media using spatially offset Raman spectroscopy, Appl. Spectrosc. 59 (12) (2005) 1485–1492, https://doi.org/10.1366/000370205775142548.
[42] M. Baranska, H. Schulz, R. Baranski, T. Nothnagel, L.P. Christensen, In situ simultaneous analysis of polyacetylenes, carotenoids and polysaccharides in carrot roots, J. Agric. Food Chem. 53 (17) (2005) 6565–6571, https://doi.org/10.1021/jf0510440.
[43] S. Kolašinac, I. Pećinar, D. Danojević, S. Aćić, Z.D. Stevanović, Raman spectroscopic-based chemometric modeling in assessment of red pepper ripening phases and carotenoids accumulation, J. Raman Spectrosc. 52 (9) (2021) 1598–1605, https://doi.org/10.1002/jrs.6197.
[44] R. Khodabakhshian, Feasibility of using Raman spectroscopy for detection of tannin changes in pomegranate fruits during maturity, Sci. Hortic. 257 (2019) 108670, https://doi.org/10.1016/j.scienta.2019.108670.
[45] S. Bruni, V. Guglielmi, F. Pozzi, A.M. Mercuri, Spatially-enhanced Raman spectroscopy (SERS) on silver colloids for the identification of ancient textile dyes. Part II: pomegranate and sumac, J. Raman Spectrosc. 42 (3) (2011) 465–473, https://doi.org/10.1002/jrs.2736.
[46] N. Santha, K.G. Sudha, K.P. Vijayakumari, V.U. Nayar, A.S. Moorthy, Raman and infrared spectra of starch samples of sweet potato and cassava, Chem. Sci. J. 102 (5) (1990) 705–712, https://doi.org/10.1007/BF03040801.
[47] A. Saletnik, B. Saletnik, C. Puchalski, Raman method in identification of species and varieties, assessment of plant maturity and crop quality - a review, Molecules 27 (14) (2022) 4454, https://doi.org/10.3390/molecules27144454.
[48] S. Mazurek, R. Szostak, A. Kita, Application of infrared reflection and Raman spectroscopy for quantitative determination of fat in potato chips, J. Mol. Struct. 1126 (2016) 213–218, https://doi.org/10.1016/j.molstruc.2016.01.064.
[49] E. Fraga, G.R. Loppnow, The role of specific amino acid residues in the vibrational properties of plastocyanin, J. Phys. Chem. B. 106 (40) (2002) 10474–10481, https://doi.org/10.1021/jp014547r.
[50] Q.S. Martins, C.A. Aguirre, J.L. Faria, Approach by Raman and infrared spectroscopy in three vegetable oils from the Brazilian Amazon, Rev. Mex. De. física 65 (4) (2019) 328–332, https://doi.org/10.31349/revmexfis.65.328.
[51] K. Balci, S. Akyuz, A vibrational spectroscopic investigation on benzocaine molecule, Vib. Spectrosc. 48 (2) (2008) 215–228.
[52] K.Y. Noonan, L.A. Tonge, O.S. Fenton, D.B. Damiano, K.A. Frederick, Rapid classification of simulated street drug mixtures using Raman spectroscopy and principal component analysis, Appl. Spectrosc. 63 (7) (2009) 742–747.
[53] C.A. Penido, L. Silveira Jr, M.T. Pacheco, Quantification of binary mixtures of cocaine and adulterants using dispersive Raman and FT-IR spectroscopy and principal component regression, Instrum. Sci. Technol. 40 (5) (2012) 441–456, https://doi.org/10.1080/10739149.2012.686356.
[54] D. Wang, L.M. Hamm, R.J. Bodnar, P.M. Dove, Raman spectroscopic characterization of the magnesium content in amorphous calcium carbonates, J. Raman Spectrosc. 43 (4) (2012) 543–548.
[55] E.M. Ali, H.G. Edwards, M.D. Hargreaves, I.J. Scowen, In situ detection of cocaine hydrochloride in clothing impregnated with the drug using benchtop and portable Raman spectroscopy, J. Raman Spectrosc. 41 (9) (2010) 938–943.
[56] T.M. Bedward, L. Xiao, S. Fu, Application of Raman spectroscopy in the detection of cocaine in food matrices, Aust. J. Forensic Sci. 51 (2) (2019) 209–219, https://doi.org/10.1080/00450618.2017.1356867.
[57] J.C. Carter, W.E. Brewer, S.M. Angel, Raman spectroscopy for the in-situ identification of cocaine and selected adulterants, Appl. Spectrosc. 54 (12) (2000) 1876–1881.
[58] C.A. de Oliveira Penido, M.T. Pacheco, I.K. Lednev, L. Silveira Jr, Raman spectroscopy in forensic analysis: identification of cocaine and other illegal drugs of abuse, J. Raman Spectrosc. 47 (1) (2016) 28–38.
[59] C. Eliasson, N.A. Macleod, P. Matousek, Non-invasive detection of cocaine dissolved in beverages using displaced Raman spectroscopy, Anal. Chim. Acta 607 (1) (2008) 50–53.
[60] Hargreaves, M.D., Page, K., Munshi, T., Tomsett, R., Lynch, G. and Edwards, H.G., 2008. Analysis of seized drugs using portable Raman spectroscopy in an airport environment—a proof of principle study. Journal of Raman Spectroscopy: An International Journal for Original Work in all Aspects of Raman Spectroscopy, Including Higher Order Processes, and also Brillouin and Rayleigh Scattering, 39 (7), pp.873–880.
[61] C.A. de Oliveira Penido, M.T. Pacheco, I.K. Lednev, L. Silveira Jr, Raman spectroscopy in forensic analysis: identification of cocaine and other illegal drugs of abuse, J. Raman Spectrosc. 47 (1) (2016) 28–38.
[62] H. Ali, R. Ullah, S. Khan, M. Bilal, Raman spectroscopy and hierarchical cluster analysis for the ingredients characterization in different formulations of paracetamol and counterfeit paracetamol, Vib. Spectrosc. 102 (2019) 112–115, https://doi.org/10.1016/j.vibspec.2019.05.002.
[63] G.R. Lakhwani, O.D. Sherikar, P.J. Mehta, Nondestructive and rapid concurrent estimation of paracetamol and nimesulide in their combined dosage form using raman spectroscopic technique, Indian J. Pharm. Sci. 75 (2) (2013) 211.
[64] L.B. Lyndgaard, F. van den Berg, A. de Juan, Quantification of paracetamol through tablet blister packages by Raman spectroscopy and multivariate curve resolution-alternating least squares, Chemom. Intell. Lab. Syst. 125 (2013) 58–66.
[65] M.A. Palafox, Raman spectrum of procaine hydrochloride, Spectrosc. Lett. 30 (6) (1997) 975–998, https://doi.org/10.1080/00387019708006701.
[66] M. De Veij, P. Vandenabeele, T. De Beer, J.P. Remon, L. Moens, Reference database of Raman spectra of pharmaceutical excipients, J. Raman Spectrosc. 40 (3) (2009) 297–307, https://doi.org/10.1002/jrs.2125.
[67] I. Martinez, C. Sanchez-Valle, I. Daniel, B. Reynard, High-pressure and high-temperature Raman spectroscopy of carbonate ions in aqueous solution, Chem. Geol. 207 (1-2) (2004) 47–58.